RTP4 Enhances Corneal HSV-1 Infection in Mice With Type 2 Diabetes Mellitus

Yunhai Dai,[1,2] Shilan Mao,[1] Xinyi Zang,[1,2] Hongqi Ge,[1] Jing Feng,[1] Yalin Wang,[3] Xia Qi,[1] Lingling Yang,[1] Qingjun Zhou,[1] and Xiaolei Wang[1]

[1]State Key Laboratory Cultivation Base, Shandong Provincial Key Laboratory of Ophthalmology, Eye Institute of Shandong First Medical University, Qingdao, China
[2]Qingdao Eye Hospital of Shandong First Medical University, Qingdao, China
[3]Department of Neurology, The First Affiliated Hospital of Shandong First Medical University & Shandong Provincial Qianfoshan Hospital; Shandong Institute of Neuroimmunology, Shandong Key Laboratory of Rheumatic Disease and Translational Medicine, Jinan, China

Correspondence: Xiaolei Wang, Qingdao Eye Hospital of Shandong First Medical University, 5 Yan'erdao Rd., Qingdao 266071, China; xiaoleishengji@163.com.

Received: April 26, 2024
Accepted: September 4, 2024
Published: September 23, 2024

Citation: Dai Y, Mao S, Zang X, et al. RTP4 enhances corneal HSV-1 infection in mice with type 2 diabetes mellitus. *Invest Ophthalmol Vis Sci*. 2024;65(11):36. https://doi.org/10.1167/iovs.65.11.36

Purpose. The purpose of this study was to investigate whether corneal lesions in mice with type 2 diabetes mellitus (T2D) infected with herpes simplex virus (HSV)-1 are more severe, and to elucidate the specific underlying mechanism.

Methods. The corneas of control mice and T2D mice induced by a high-fat diet combined with streptozotocin were infected with the HSV-1 Mckrae strain to assess corneal infection, opacity, and HSV-1 replication. RNA sequencing of the corneal epithelium from wild-type and db/db mice (a genetic T2D mouse model) was conducted to identify the key gene affecting T2D infection. Immunofluorescence staining was performed on corneal sections from T2D mice and patients with T2D. The effect of small interfering RNA (siRNA) knockdown on corneal HSV-1 infection was evaluated in both in vitro and in vivo models.

Results. T2D mice exhibited a more severe infection phenotype following HSV-1 infection, characterized by augmented corneal opacity scores, elevated viral titers, and transcripts compared to control mice. Transcriptome analysis of corneal epithelium revealed a hyperactive viral response in T2D mice, highlighting the differentially expressed gene *Rtp4* (encoding receptor transporter protein 4). Receptor transporter protein 4 (RTP4) expression was enhanced in the corneal epithelium of T2D mice and patients with T2D. Virus binding assays demonstrated that RTP4 facilitated HSV-1 binding to human corneal epithelial cells. Silencing RTP4 alleviated HSV-1 infection in both in vitro and in vivo T2D models.

Conclusions. The findings indicate that elevated RTP4 exacerbates HSV-1 infection by enhancing its binding to corneal epithelial cells, whereas *Rtp4* knockdown mitigated corneal lesions in T2D mice. This implies RTP4 as a potential target for intervention in diabetic HSV-1 infection.

Keywords: receptor transporter protein 4 (RTP4), cornea, type 2 diabetes (T2D), herpes simplex virus (HSV)-1, herpes simplex keratitis (HSK)

Herpes simplex virus (HSV)-1, a member of the alpha subfamily of herpesviruses, is a globally widespread infectious human virus that causes herpes simplex keratitis (HSK) in the cornea.[1,2] HSK often leads to visual impairment and even blindness, and is a leading cause of infectious blindness.[3,4] Type 2 diabetes mellitus (T2D), the largest global epidemic, is a predisposing factor for HSK,[5,6] with other risk factors, including immunodeficiency, ultraviolet radiation exposure, and topical corticosteroids.[1,7] However, the effect and mechanism of T2D on HSK remain largely unexplored.

The receptor transporter protein 4 (RTP4), a member of the RTP family, is originally identified as a molecular chaperone of a group of G-protein–coupled receptors that facilitates their transport to the cell surface to mediate a bitter taste sense.[8] Accumulating evidence indicates RTP4 is implicated in innate immune regulation and viral response.[9–11] The antiviral properties of RTP4 have been unveiled in a variety of RNA viruses, including severe acute respiratory syndrome-coronavirus 2 (SARS-CoV-2), Zika virus, hepatitis C virus, yellow fever virus, and dengue virus.[9,11,12] By contrast, He et al. found that RTP4 negatively regulates IFN-I responses by modulating cGAS-STING signaling, thereby exacerbating symptoms of experimental cerebral malaria and increasing West Nile viral load in mouse brains, suggesting that RTP4 may indirectly contribute to parasite growth and viral infection.[10] Little is known about the role of RTP4 in DNA virus infection, with the exception of findings by Boy et al., who reported that ectopic expression of RTP4 in vivo has no inhibitory effect on the DNA virus HSV-1,

despite RTP4 effectively inhibiting RNA viruses, such as Zika virus, yellow fever virus, and dengue virus.[9] In this study, we investigated the role of RTP4 in mouse corneal HSV-1 infection. We observed that RTP4 expression was elevated in the corneal epithelium of both diabetic mice and patients with diabetes, however, the specific role of this upregulation remains unclear.

In our study, we demonstrated that T2D exacerbated corneal HSV-1 infection, and further found that enhanced RTP4 expression mediated severe corneal lesion following HSV-1 infection in T2D mice. Knockdown of *Rtp4* mitigated HSV-1 infection in both the T2D cell model and corneas of T2D mice, suggesting that RTP4 serves as a potential therapeutic target for diabetic HSV-1 infection.

Materials and Methods

Animals Models and Human Tissues

T2D Murine Models. Male C57BL/6 mice (8 weeks old) were purchased from Vital River Laboratory (Beijing, China). Streptozotocin (STZ) is an antibiotic, and STZ combined with a high-fat diet (HFD) is widely used to establish a model of T2D.[13] The ingestion of HFD triggers insulin resistance and induces obesity, and subsequent multiple injections of low-to-moderate doses of STZ lead to sustained autoimmune destruction of β-cells, producing mild-to-moderate insulin deficiency, which accelerates the progression of T2D in mice.[14,15] To establish a T2D mouse model, a modified protocol from previous studies was followed.[14–16] Mice were subjected to intraperitoneal injection of STZ at a dosage of 60 mg/kg/day (MCE, Shanghai, China), dissolved in sodium citrate buffer (0.1 mmol/L, pH 4.5), administered for 5 consecutive days following 4 weeks of an HFD (Beijing Keao Xieli Feed Co., Ltd., D12451, 45% fat), and were subsequently maintained on the HFD. Control mice were fed a standard diet (Beijing Keao Xieli Feed Co., Ltd., D12450B, 10% fat) and received vehicle injections. After 2 weeks post-final injection, measurements of body weight, blood glucose, and blood lipid levels were conducted in both groups of mice.

C57 BL/KS db/db male mouse ($Lepr^{db/db}$) is an inherited murine model of T2D that carries a mutation in the gene encoding the leptin receptor, resulting in dysfunctional leptin signaling.[17,18] C57 BL/KS db/db male mice ($Lepr^{db/db}$, 8 weeks old) and age-matched wild-type (WT) male mice ($Lepr^{+/+}$) were obtained from GemPharmatech (Strain NO. T002407; Nanjing, China). Fed a standard chow diet without HFD/STZ treatment, db/db mice spontaneously exhibit typical symptoms of T2D.[17,18] After 4 weeks on a standard diet, RNA sequencing was conducted on the corneal epithelia of db/db and WT mice.

All animal experiments were approved by the Ethics Committee of Shandong Eye Institute and conducted in compliance with the ARVO Statement for the Use of Animals in Ophthalmic and Vision Research.

Human Samples. Healthy and T2D human corneas were sourced from the eye bank of Qingdao Eye Hospital. Detailed information for each patient and donor is provided in Supplementary Table S1. This study was approved by the Ethics Committee of Shandong Eye Institute (code 2023-35).

RNA Sequencing Assay. Corneal epithelium from db/db and WT mice was collected using a corneal epithelial scraper and sent to LC-BIO Co., Ltd. (Hangzhou, China) for RNA sequencing. Each sample comprised the corneal epithelium from two eyes of a mouse, with three samples per group. Volcano and heat maps were generated using the OECloud tools, accessible at https://cloud.oebiotech.com. Gene ontology (GO) enrichment analysis and enrichment cnetplot were conducted at http://www.bioinformatics.com.cn/.

HSV-1 Virus and Murine HSK Model. The Mckrae strain of HSV-1 was presented by Professor Jumin Zhou of Kunming Institute of Zoology, China. HSV-1 was propagated and titered on Vero cells, as previously described.[19]

To establish the HSK model, control and T2D mice were anesthetized with intraperitoneal injection of 0.6% pentobarbital sodium. Corneal scratching was performed using a 30G needle, as described previously,[19–21] followed by administration of HSV-1 at a titer of 1×10^6 pfu (5 µL). The MOCK group received 5 µL of DMEM/F-12 medium (2% fetal bovine serum [FBS]). Treatment was applied to the right eye of each mouse, whereas the left eye remained intact.

The titer of HSV-1 was determined using a plaque assay. Briefly, viral samples were obtained by swabbing the murine eyes with sterile cotton swabs at indicated time points. The prepared Vero monolayer cells in 24-well plates were then infected with the collected viral solutions through serial dilutions. Following an incubation period of 3 or 4 days, the cells were fixed and stained with crystal violet (Beyotime). Finally, plaques were counted and graphed, and the virus titers were calculated.

Corneal Evaluation

Corneal alterations in both control and T2D mice were photographed under a BQ 900 slit lamp (Haag-Streit, Bern, Switzerland) at specified time points. Corneal opacity was graded as our previous description: 0, 1, 2, 3, 4, and 5 for transparent, mildly cloudy, moderate opacity, severe opacity, most severe opacity, and corneal perforation, respectively.[19]

Cell Culture, Treatment, and Cell Viability Assay

Human corneal epithelial cells (HCECs) were cultured in Dulbecco's modified Eagle's medium (DMEM)/F12 medium (17.2 mmol/L glucose) with 10% FBS. To induce an in vitro T2D model, HCECs were treated with DMEM medium (25 mmol/L glucose) supplemented with palmitate (PA), as previously described.[22] The cell viability assay was carried out as previously reported with minor modifications.[23] Briefly, HCECs were plated in 96-well plates and treated with PA at various concentrations (0, 100, 200, 300, 400, and 600 µmol/L) until reaching 70% to 80% confluence for 24 hours. Following incubating with CCK-8 (Beyotime, Shanghai, China), the absorbance was measured using a microplate reader (SpectraMax M2; Molecular Devices, Menlo Park, CA, USA). Relative cell viability was calculated according to the manufacturer's instructions, comparing values to the vehicle group after subtracting the background.

Assays of HSV-1 Binding and Replication

Assays of HSV-1 binding and replication were performed as previously described.[24,25] In virus binding assays, HCECs were infected with a H129-G4 HSV-1 strain virus expressing GFP (Genechem, Shanghai, China) at 4°C for 2 hours with 1 MOI. After washing with cold PBS buffer, fixing, and

Investigative Ophthalmology & Visual Science

Table. The Specific Primers for Quantitative PCR

Name	Forward Primer 5′-3′	Reverse Primer 5′-3′
ICP0	GCCCACTACACCAGCCAATC	AGACAGCAAAAATCCCCTGAGTT
TK	AAGGTCGGCGGGATGAG	CGGCCGCGCGATAC
VP16	GCGGGGCCGGGATTTACC	CTCGAAGTCGGCCATATCCA
HSV-1	GCCCGTGGTTCTGGAATTC	GATGTTGTACCCGGTCACGAA
m-Rpl5	CCGCAGGCTTCTGAATAGGT	CCAGTTGTAGTTCGGGCAAGA
m-Rtp4	ATGCATCTTTGGGTGAGAAGGT	GGGAGGAACTCTTTGGTAATGGA
m-Ifitm3	TGTGATCAACATGCCCAGAGA	CAGTCACATCACCCACCATCTT
m-Isg15	GCCTGGGACCTAAAGGTGAAG	TCCTGGAGCACTGCAGTTTG
m-Oas1a	GGAGCTCCAGCGGAACTTC	CAGGCAAAGACAGTGAGCAACT
m-Oas2	CCAACCAATAATGTGGGCAAA	GTGGCTTGGAGTGACGAAAAG
m-Oas3	ATAAACACTTGCCCTCCCAAAC	CTTTTGCTCTCCACAGCCTTGT
m-Oasl2	GCAGGTCTGTTGCACGACTGT	GATCTCTGCCTTCATCTTTCTGATG
m-Usp18	TCCCTCAGAGCTTGGATTTCA	TCCGGATGTAGGCACAGTAATG
m-Zbp1	AGTGCCCAAGAAAACCCTCAAT	CTAGGCTGGGCACTGGAGTT
m-Irf7	CACCCCCATCTTCGACTTCA	TCACCAGGATCAGGGTCTTCTC
m-β-actin	GGCACCACACCTTCTACAATG	GTGGTGGTGAAGCTGTAGCC
h-ZO-1	AGGATCCATATCCCGAGGAA	CGAGGTCTCTGCTGGCTTGT
h-ATP1A1	CAGGGCAGTGTTTCAGGCTA	TCGACGATTTTGGCGTATCTT
h-β-actin	GCAGAAGGAGATCACTGCCCT	GCTGATCCACATCTGCTGGAA
h-Rtp4	TGGCTGGTTCCGGTGTTC	TGGGACCAGGAGCACTTCTG

DAPI staining, the cells were observed using a forward and inverted integrated fluorescence microscope (Revolve RVL-100; Echo Laboratories, San Diego, CA, USA). The viral replication assays were performed by quantitative PCR after incubation at 37°C for 24 hours following the binding assay.

Rtp4 Knockdown In Vitro and In Vivo

For knocking down *Rtp4* in HCEC cells, 50 nM *Rtp4* small interfering RNAs (siRNAs) or negative control (NC) siRNA were transfected into HCEC cells with Lipofectamine 3000 (Thermo Fisher Scientific, Waltham, MA, USA) according to the manufacturer's instructions. The siRNA target sites specific for human *Rtp4* were as follows: *Rtp4* siRNA-1: 5′-CCATGAGGATTCTGAGCAA-3′, *Rtp4* siRNA-2: 5′-GCTCAAGGGTGGAAGCAAT-3′, and *Rtp4* siRNA-3: 5′-CTGGAAGGATCCCATGACA-3′. The NC siRNA was provided by RiboBio Company (Guangzhou, China).

To knock down *Rtp4* in mouse corneas, 10 µM (5 µL per cornea) methoxy-modified mouse *Rtp4* siRNA or negative control (NC) siRNA was subconjunctivally injected into T2D mice. Injections were administered every other day for a total of three times. The siRNA target site specific for mouse *Rtp4* was as follows: m-*Rtp4* siRNA: 5′-CCATGAGGATTCTGAGCAA-3′.

Real-Time Quantitative PCR

Total RNAs from mouse corneal epithelium, stroma, whole cornea, and HCEC cells were extracted using a TransZol Up Plus RNA Kit (ER501-01-V2; Transgen, Beijing, China), respectively. Corneal epithelium was separated from stroma and endothelium after overnight digestion at 4°C using Dispase II (Roche, Indianapolis, IN, USA), with endothelium removed by tweezers. After the synthesis of complementary DNAs, real-time quantitative PCR was performed using SYBR Green reagents (Q711-03; Vazyme) and analyzed by the Applied Biosystems 7500 Real-Time System (Applied Biosystems, Foster City, CA, USA). The specific primers are listed in the Table.

Hematoxylin and Eosin Staining

Mouse corneas were fixed, embedded in paraffin, and sectioned into 4 µm thickness. Hematoxylin and eosin (H&E) staining was performed as described previously.[26] Sections were observed and images were captured using a light microscope (Nikon, Tokyo, Japan).

Immunofluorescence Staining

For cryosection immunofluorescence staining, mouse eyeballs were collected at the indicated time points and embedded in Tissue-Tek OCT (Sakura Finetek, Tokyo, Japan), then sectioned into 7 µm thickness. For cell immunofluorescence staining, HCEC cells were washed with PBS and fixed in 4% paraformaldehyde. Immunofluorescence staining was performed as in our previous description.[26,27] The antibodies used were as follows: FITC-conjugated CD45 (2607666; Invitrogen, eBioscience, San Diego, CA, USA), RTP4 (PA5-113215; Invitrogen, USA), ICP4 (sc-69809; Santa Cruz Biotechnology Inc., Dallas, TX, USA), ZO-1 (40-2200; Invitrogen, USA), and ATP1A1 (MA3-929; Invitrogen, USA). Sections were incubated overnight with primary antibody at 4°C, followed by the appropriate secondary antibody for 2 hours. All sections were observed under a ZEISS LSM880 inverted microscope (ZEISS, Rossdorf, Germany) after counterstaining with DAPI.

Immunofluorescence of paraffin sections was performed according to our previous report with minor modifications.[28] Briefly, sections of human samples were dewaxed, hydrated, and antigen retrieved with sodium citrate buffer (10 mM sodium citrate, 0.05% Tween 20, and pH 6.0). After natural cooling, the sections were rinsed, blocked, and incubated with the primary antibody RTP4 (PA5-113215; Invitrogen, USA) at 4°C overnight, following the same steps as above.

Western Blot

After treatment with the aforementioned siRNAs, mouse corneas and HCECs were harvested separately at the indi-

Investigative Ophthalmology & Visual Science

cated time points. Total proteins were extracted using radioimmunoprecipitation assay (RIPA) buffer supplemented with cOmplete protease inhibitor (Roche). The primary antibodies utilized in this study were RTP4 (Invitrogen) and β-Actin (Proteintech, Wuhan, China). Blots were incubated with a horseradish peroxidase (HRP)–conjugated secondary antibody (Proteintech) and visualized through enzyme-linked chemiluminescence using the Immobilon Western HRP substrate (Millipore, Billerica, MA, USA) and ChemiDoc Touch (Bio-Rad, Hercules, CA, USA).

Statistical Analysis

Data are expressed as mean ± standard deviation (SD). Statistical analysis was performed by GraphPad software. Statistical significance was assessed by the unpaired two-tailed Student's *t*-test, and by 1-way analysis of variance (ANOVA; a comparison of more than 2 groups) and 2-way ANOVA (for comparison of 2 independent variables such as control and T2D, MOCK, and HSV-1) by GraphPad Prism software. Any P values < 0.05 was considered statistically significant. All experiments were performed at least three times.

Results

T2D Exacerbates HSV-1 Infection

To investigate the effect of T2D on HSV-1 infection, we established a T2D mouse model induced by HFD and STZ, as illustrated in Figure 1A. T2D mice exhibited noticeable differences compared to control mice, including increased body weight and significantly elevated levels of blood glucose and blood lipids (see Figs. 1B–D). Following HSV-1 infection, slit-lamp examination and cornea opacity scoring manifested aggravating symptoms in T2D mice. At 1 day post-infection (Dpi), T2D mice displayed mild inflammation and opacity in the cornea, whereas control mice showed nearly transparent corneas. By 3 Dpi, T2D mice exhibited a larger corneal infection area compared to controls, and by 5 Dpi, severe edema and opacity encompassed the entire cornea of T2D mice (see Figs. 1E, 1F). At 7 Dpi, T2D mice exhibited elevated corneal opacity scores and noticeable vascular invasion compared to the control group (Figs. 1E, 1F). Eye swabs were collected from the mice at 3, 5, and 7 Dpi for plaque analysis. Our results showed that the viral titers at both 3 and 5 Dpi in T2D mice were significantly higher than those in control mice

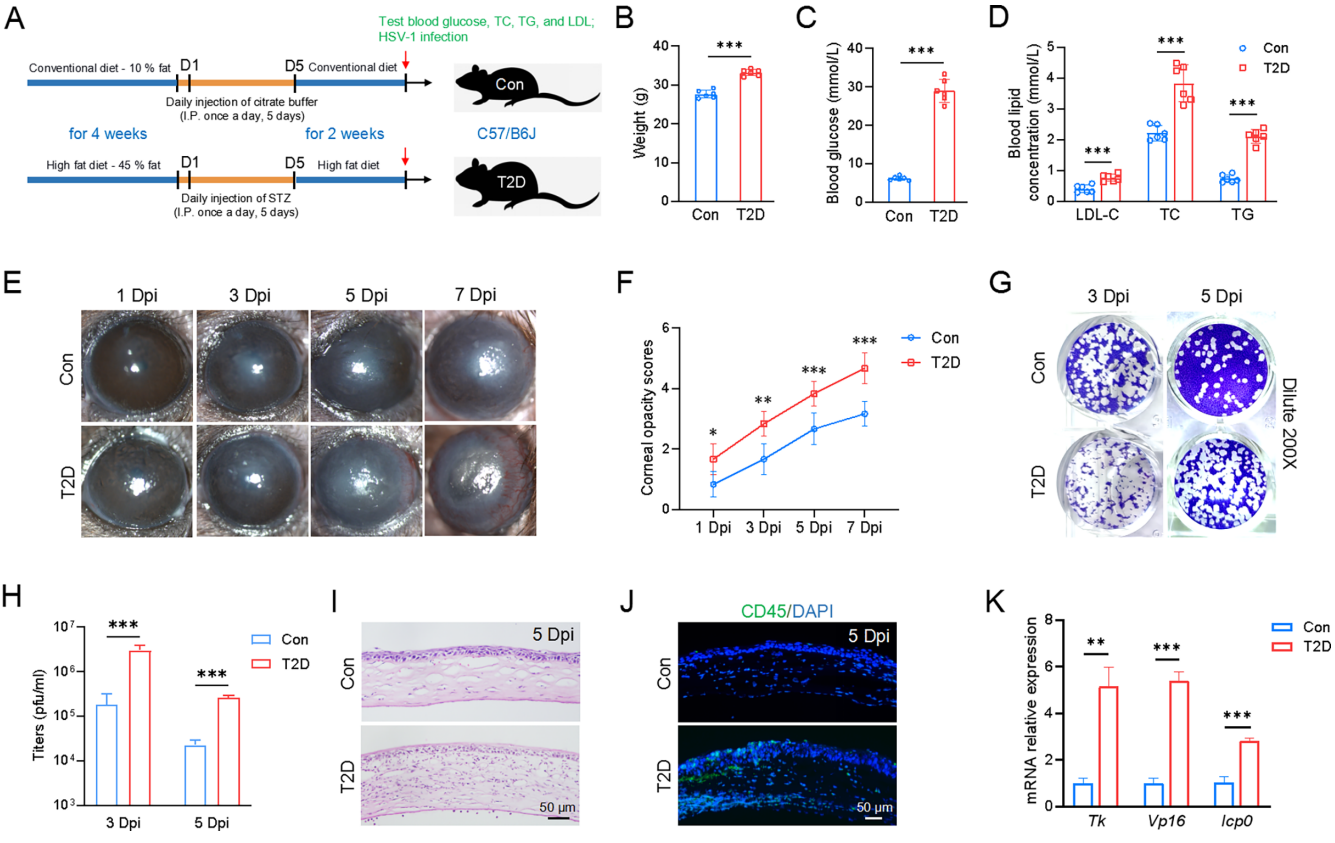

Figure 1. Increased susceptibility of T2D mice to HSV-1 infection. (**A**) Schematic illustrating the generation of T2D mice. (**B–D**) Compared to control mice, T2D mice had higher body weight, blood glucose levels, and blood lipid levels. LDL-C, low density lipoprotein cholesterol; TC, total cholesterol; TG, triglyceride ($N = 6$ per group). (**E**) Slit-lamp images demonstrated that T2D mice had a more severe corneal phenotype than control mice following HSV-1 infection. Dpi, days post infection. (**F**) Corneal opacity scores were significantly high in T2D mice compared to control mice ($n = 6$ per group). (**G**) Representative images of plaque assay at 3 and 5 Dpi. The viral samples were diluted 200 times. (**H**) Virus titers in T2D mice were clearly higher than those in the control mice ($n = 3$ per group). (**I**) H&E staining of corneal sections ($n = 3$ per group). (**J**) More immune cells infiltrated the cornea of T2D mice ($n = 3$ per group). (**K**) Quantitative PCR analysis of HSV-1 viral genes (*Tk*, *Vp16*, and *Icp0*). Mouse *Rpl5* (*m-Rpl5*) was used as an internal control ($n = 3$ per group). *$P < 0.05$, **$P < 0.01$, ***$P < 0.001$.

Investigative Ophthalmology & Visual Science

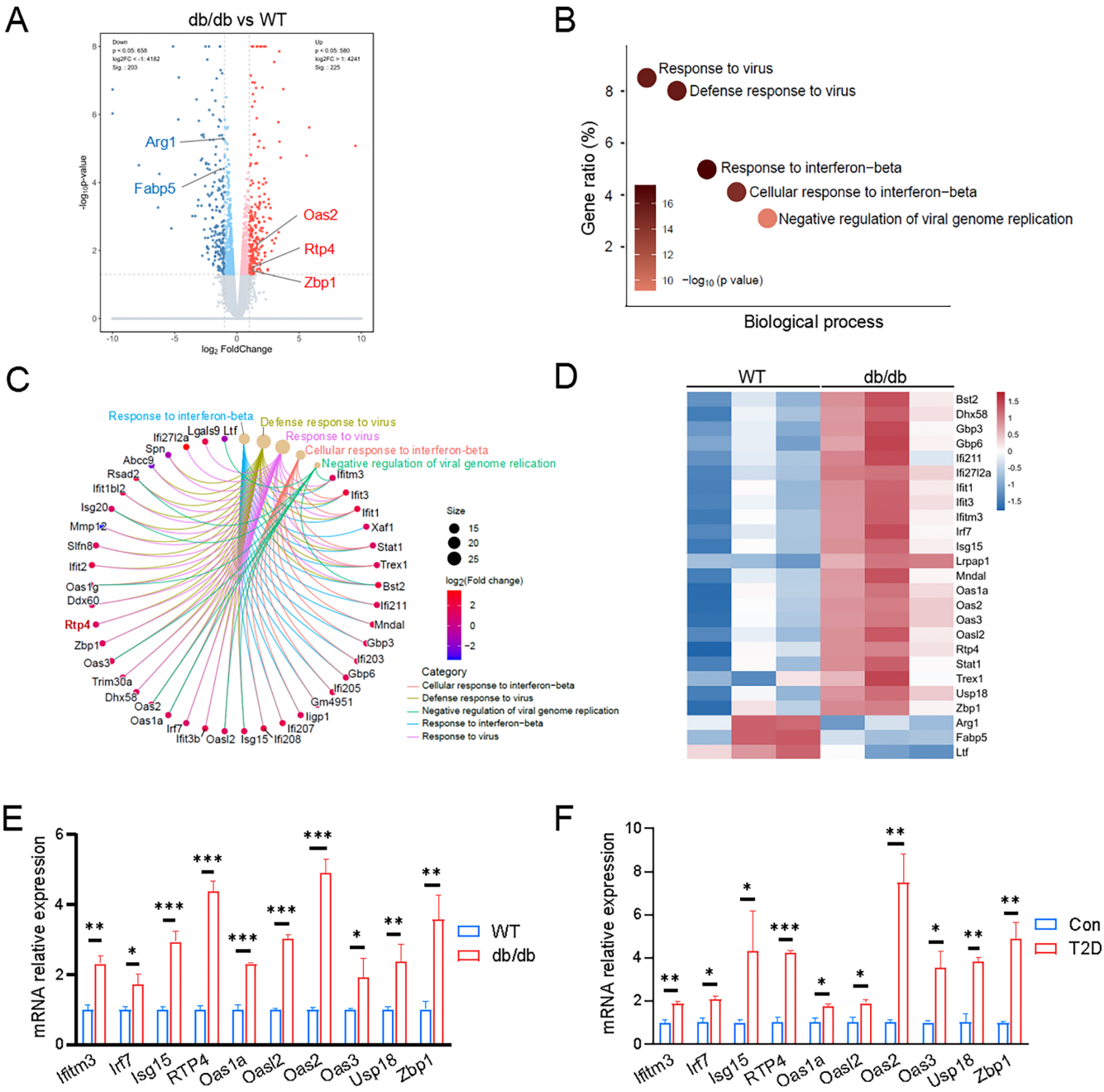

Figure 2. Enhanced virus response genes expression in corneal epithelium of db/db mice and T2D mice. (**A**) Volcano plot illustrates the differential mRNA expression profile of corneal epithelia between WT and db/db mice. (**B**) Top five terms of the GO biological process enrichment analysis of significantly dysregulated genes in the corneal epithelium. (**C**) The cnetplot visualization depicts the enrichment of dysregulated genes from the top five enriched categories. (**D**) Heat map of representative virus response-related genes. (**E**, **F**) Quantitative PCR analysis validates the enhanced expression of virus response genes in corneal epithelia of both db/db and T2D mice, compared to controls. *m-β-actin* served as an internal control. $^{*}P < 0.05$, $^{**}P < 0.01$, $^{***}P < 0.001$.

(Figs. 1G, 1H). However, by 7 Dpi, the viral titers were very low in both T2D and control mice, with no plaque formation observed (Supplementary Fig. S1). Given that the differences in corneal phenotype and viral replication between the 2 groups were most pronounced at 5 Dpi, we selected this time point for subsequent experiments. Furthermore, H&E staining and immunofluorescence staining showed significant corneal thickening and abundant infiltration of inflammatory cells (CD45+) in T2D mice (see Figs. 1I, 1J). Quantitative PCR analysis demonstrated elevated expression levels of viral replication-related genes, including thymidine kinase (TK), tegument protein VP16, and immediate early protein ICP0, in T2D mice compared to controls (see Fig. 1K). There was no significant difference between the MOCK treatment of control and T2D mice, both of which showed clear corneas (Supplementary Fig. S2). These results indicated that T2D aggravated corneal HSV-1 infection.

Investigative Ophthalmology & Visual Science

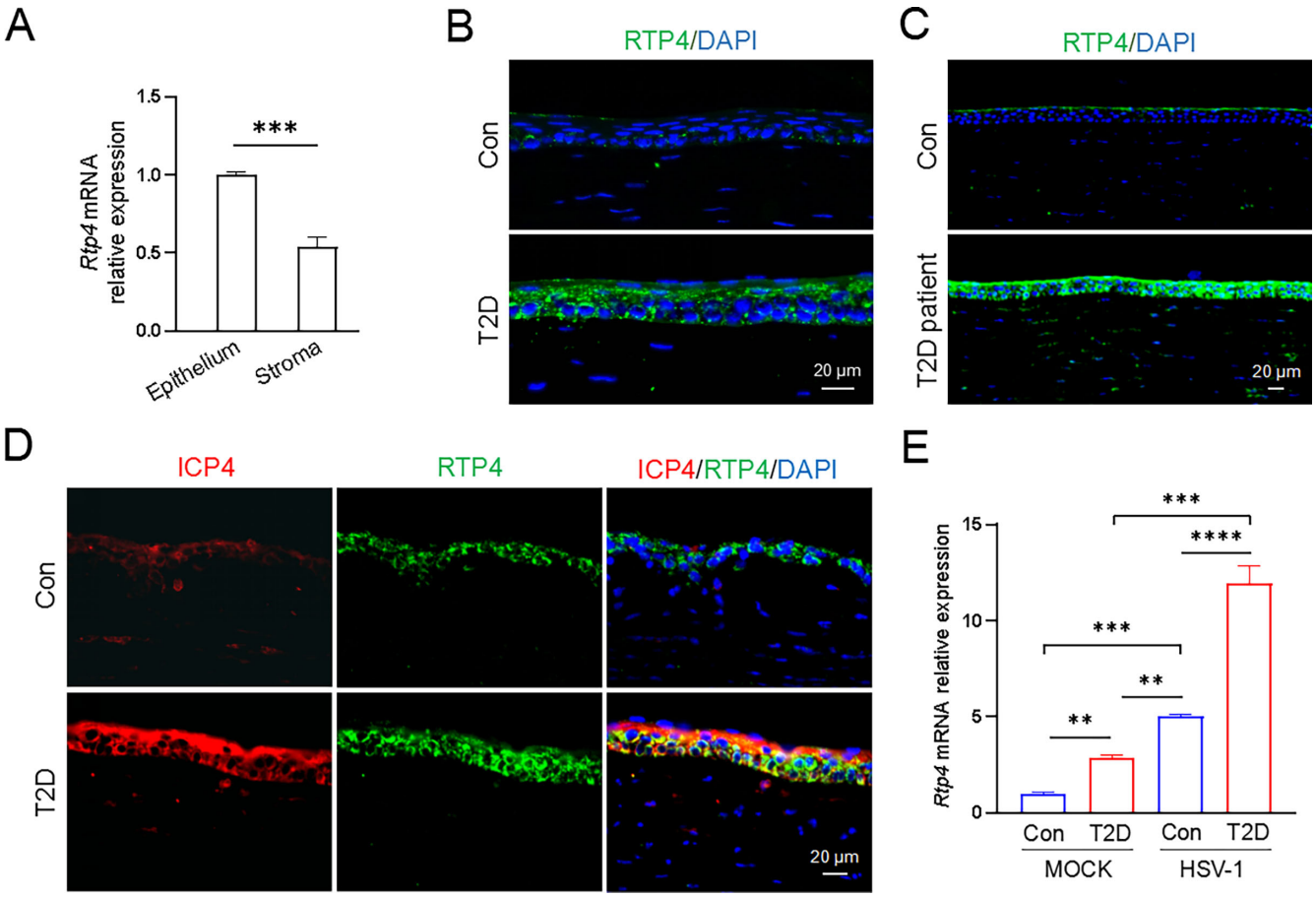

Figure 3. Involvement of upregulated RTP4 in corneal HSV-1 infection in T2D mice. (**A**) Quantitative PCR results showed that *Rtp4* had a higher expression level in murine corneal epithelium than corneal stroma. (**B**, **C**) Representative images of RTP4 staining in control and T2D mice, and healthy donors and patients with T2D ($n = 3$ per group). (**D**) Representative pictures of ICP4 and RTP4 staining in control and T2D mice at 5 Dpi ($n = 3$ per group). (**E**) Quantitative PCR analysis of *Rtp4* gene expression in murine corneas. MOCK, without HSV-1 infection; HSV-1, at 5 Dpi. $^{**}P < 0.01$, $^{***}P < 0.001$.

The Hyperactive Virus Response Signaling in the Corneal Epithelium of T2D Mice

It is widely known that both db/db mice and HFD/STZ-induced mice are typical animal models mimicking human T2D. Given the simplicity and stability of db/db mice in modeling T2D, we conducted transcriptome sequencing on the corneal epithelium ($n = 3$) from both WT and db/db mice to interrogate the pathogenesis underlying the susceptibility of T2D to HSV-1 infection. Comparative expression analysis unveiled 428 differentially expressed genes (fold change > 2, $P < 0.05$) in the corneal epithelium of db/db mice compared with WT mice. Among these, 225 genes were significantly upregulated, whereas 203 genes were significantly downregulated (Fig. 2A). GO biological process enrichment analysis highlighted virus-related categories, such as response to virus, defense response to virus, and response to interferon-beta, as the most significantly altered in the corneal epithelium of T2D mice (see Fig. 2B). The enrichment cnetplot depicted dysregulated genes of the top five enriched categories (see Fig. 2C). The heat map further illustrated that signature genes associated with viral infection and innate immune response, including *Ifitm3*, *Irf7*, *Isg15*, *Rtp4*, *Oas1a*, *Oasl2*, *Oas2*, *Oas3*, *Usp18*, and *Zbp1*, were significantly upregulated in db/db mice compared to WT mice (see Fig. 2D). Quantitative PCR validation confirmed the significant upregulation of the aforementioned genes in the corneal epithelium of db/db mice (see Fig. 2E), consistent with the quantitative PCR result of corneal epithelium from STZ-mediated T2D mice (see Fig. 2F). These findings indicated an abnormal viral response in the corneal epithelium of db/db mice and STZ-mediated T2D mice, potentially associated with HSV-1 infection.

Noticeably, among genes associated with viral infection and innate immune response, *Rtp4* was highly upregulated and most significant in the corneas of both db/db mice and STZ-mediated T2D mice compared with their respective controls. Quantitative PCR results showed that *Rtp4* was increased by 4.393 ± 0.278-fold ($P = 0.0007$) and 4.24 ± 0.114-fold ($P = 0.0002$) in db/db mice and STZ-mediated T2D mice, respectively (see Figs. 2E, 2F). This suggests that RTP4 may be involved in corneal HSV-1 infection.

RTP4 Expression Positively Correlates With Corneal HSV-1 Infection

RTP4 encodes a receptor transporter protein and modulates virus infection and immune response.[9–11] RTP4 displayed

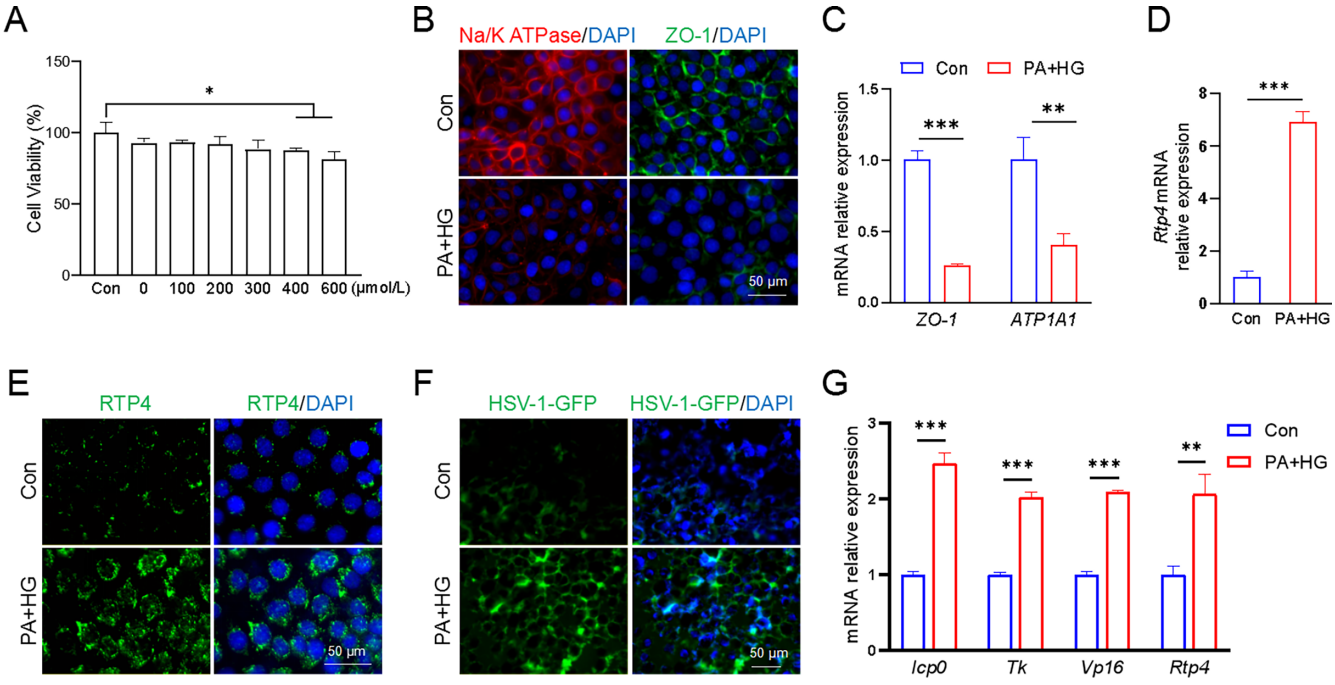

Figure 4. Both RTP4 expression and HSV-1 infection were enhanced in a T2D cell model. (**A**) Cell viability assay of HCECs treated with different PA concentrations for 24 hours. Then HCECs were treated with 300 μmol/L PA and HG medium to induce the T2D cell model, whereas HCECs were cultured in DMEM/F12 medium as a control group. (**B**) Representative immunofluorescence images of ATP1A1 and ZO-1 in control HCECs and PA + HG-treated HCECs. (**C**) Quantitative PCR analysis of *ATP1A1* and *ZO-1* gene expression. (**D**) Quantitative PCR analysis of *Rtp4* gene expression. (**E**) Representative immunofluorescence images of RTP4. (**F**) Representative images showing GFP-labeled HSV-1 infection post 24 hours. (**G**) Quantitative PCR analysis of HSV-1 viral genes and *Rtp4* gene in Figure 4F. Human *β-actin* (*h-β-actin*) served as an internal control. $^{*}P < 0.05$, $^{**}P < 0.01$, $^{***}P < 0.001$.

a higher expression level in corneal epithelium than corneal stroma of control mice (Fig. 3A). Normally, a small amount of RTP4 was found in mouse corneal epithelium (see Fig. 3B). In T2D mice, RTP4 acquired a robustly increased expression in corneal epithelium (see Fig. 3B). Likewise, immunofluorescence staining of paraffin sections showed a markedly elevated expression of RTP4 in the corneal epithelium of patients with T2D compared with normal donors (see Fig. 3C). After HSV-1 infection, there was a noticeable increase in both ICP4, an immediate early gene of HSV-1, and RTP4 in T2D mice (see Fig. 3D). Quantitative PCR assay further exhibited that RTP4 expression was enhanced by both T2D and HSV-1 infection, with its expression peaking after HSV-1 infection in T2D mice (see Fig. 3E).

To investigate the relationship between RTP4 expression and HSV-1 infection, a T2D cell model was established treated with PA and high-glucose (HG; 25 mmol/L glucose) medium. HCECs were cultured in the HG medium and exposed to various concentrations of PA for 24 hours. Cell viability was assessed, and a PA concentration of 300 μmol/L was chosen for the T2D cell model, ensuring no impact on cell viability (Fig. 4A). As previously reported,[22] the T2D cell model was confirmed by significant down-regulation of ATP1A1 and ZO-1 mRNA and protein levels (see Figs. 4B, 4C). Subsequent quantitative PCR assay and immunofluorescence staining demonstrated a clear enhancement of RTP4 in the T2D cell model compared to controls (see Figs. 4D, 4E), mirroring the findings in T2D mice (see Figs. 3B, 3C). After 24 hours of HSV-1-GFP infection, the fluorescent intensity of HSV-1 was pronouncedly increased in the T2D cell model (see Fig. 4F). Moreover, quantitative PCR assay revealed higher expression of viral replication-related genes and increased *Rtp4* expression in the T2D cell model (see Fig. 4G). Collectively, these results suggest a positive correlation between RTP4 expression and corneal HSV-1 infection, implying that RTP4 may contribute to the susceptibility of T2D mice or patients with T2D to HSV-1.

RTP4 Modulates HSV-1 Infection

To elucidate the role of RTP4 in HSV-1 infection, we utilized siRNA to knock down *Rtp4* in HCECs. Control HCECs were transfected with different *Rtp4* siRNAs for 24 hours, and quantitative PCR assay and Western blot confirmed the effective knockdown of *Rtp4* by all siRNAs (Figs. 5A, 5B). *Rtp4* siRNA-1 was selected for subsequent experiments. In the T2D cell model induced by PA + HG, immunofluorescence staining validated that siRNA successfully reduced RTP4 protein levels (see Fig. 5C). After 24 hours of HSV-1-GFP infection, T2D cells exhibited a stronger fluorescence signal compared to control cells under a fluorescence microscope, suggesting increased viral infection. *Rtp4* knockdown attenuated viral infection in both control and T2D cells (see Fig. 5D). Consistently, quantitative PCR results demonstrated that the expression of viral replication-associated genes was upregulated in the T2D group compared with the control group; whereas knockdown of *Rtp4* significantly reduced the expression of these genes in both groups (see Fig. 5E).

To determine whether RTP4 is involved in HSV-1 binding, HCECs were stored at 4°C for 2 hours under conditions that inhibit HSV-1 entry (Fig. 6A). After washing and fixation, fluorescence imaging revealed an intensified fluorescence signal of HSV-1 on the cell membrane in T2D cell models

Investigative Ophthalmology & Visual Science

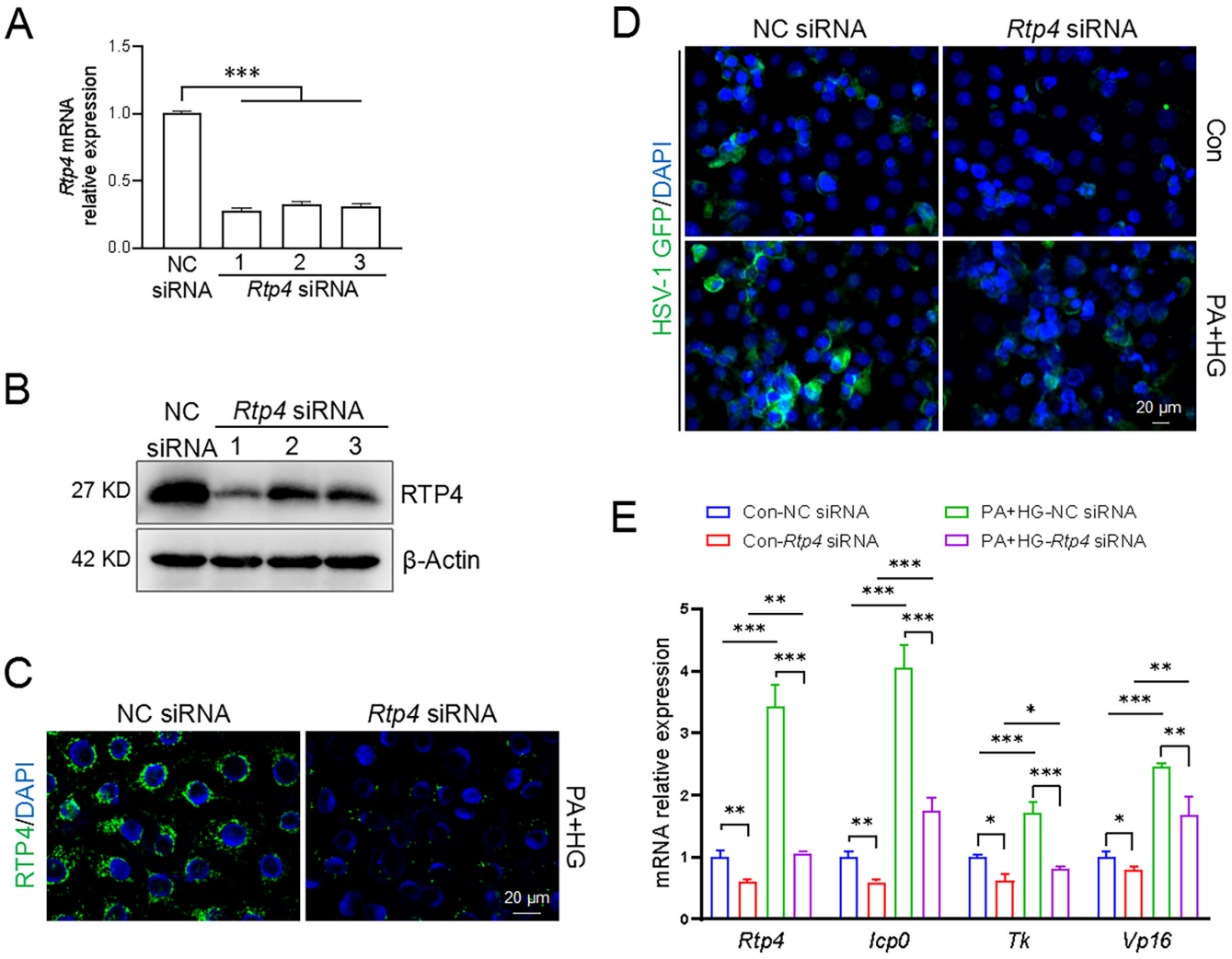

Figure 5. ***Rtp4* knockdown restricted HSV-1 infection in a T2D cell model.** Knockdown of *Rtp4* by specific siRNAs was detected by quantitative PCR and Western blot in HCECs of the control group (**A**, **B**) and immunofluorescence staining in HCECs of the T2D group (**C**). (**D**) After 24 hours of HSV-1 infection, representative images showing GFP-labeled HSV-1 infection with NC siRNA and *Rtp4* siRNA. MOI = 1. (**E**) Quantitative PCR analysis of HSV-1 viral genes and *Rtp4* gene in Figure 5C. The *h-β-actin* was used as an internal control. NC, negative control. $^{*}P < 0.05$, $^{**}P < 0.01$, $^{***}P < 0.001$.

(see Fig. 6B). This suggests that enhanced RTP4 promotes the binding of HSV-1 to HCECs. Conversely, *Rtp4* knockdown notably diminished the fluorescence signal on the cell membrane in T2D cell models (see Fig. 6D), indicating a crucial role of RTP4 in HSV-1 binding to HCECs. Following virus binding, and subsequent 24-hour incubation at 37°C, the mRNA level of HSV-1 significantly increased in the T2D cell model compared to the control group (see Fig. 6C), but decreased markedly after *Rtp4* knockdown (see Fig. 6E). Together, these results suggest RTP4 facilitates HSV-1 infection through influencing its binding to host cells.

Rtp4 Knockdown Ameliorated the Degree of HSK Lesions in T2D Mice

To assess the role of RTP4 in HSV-1 infection in vivo, we used a specific methoxy-modified siRNA to knock down *Rtp4* via subconjunctival injection. In STZ-mediated T2D mice, quantitative PCR, Western blot, and immunofluorescence staining confirmed a marked downregulation of RTP4 in the cornea (Figs. 7A–C). Topical administration of *Rtp4* siRNA to T2D mice alleviated HSV-1 infection symptoms, manifesting in a clearer cornea (see Fig. 7D), reduced corneal opacity scores (see Fig. 7E), and decreased immune cell infiltration and corneal edema compared to the NC siRNA-treated group (see Figs. 7F, 7G). Furthermore, immunofluorescence staining demonstrated that suppression of RTP4 expression led to a decrease in the protein level of ICP4, an HSV-1-associated antigen (see Fig. 7H). Consistently, after *Rtp4* knockdown in T2D mice, genes related to HSV-1 replication showed significant downregulation compared to the control group (see Fig. 7I). These data indicated that RTP4 participated in the process of corneal HSV-1 infection, and its suppression had an ameliorative effect, suggesting that RTP4 is a new intervention target for corneal HSV-1 infection.

Discussion

In this study, we found that RTP4 was mainly expressed in the corneal epithelium. Enhanced RTP4 expression was found in the corneal epithelium of both HFD/STZ-induced

Investigative Ophthalmology & Visual Science

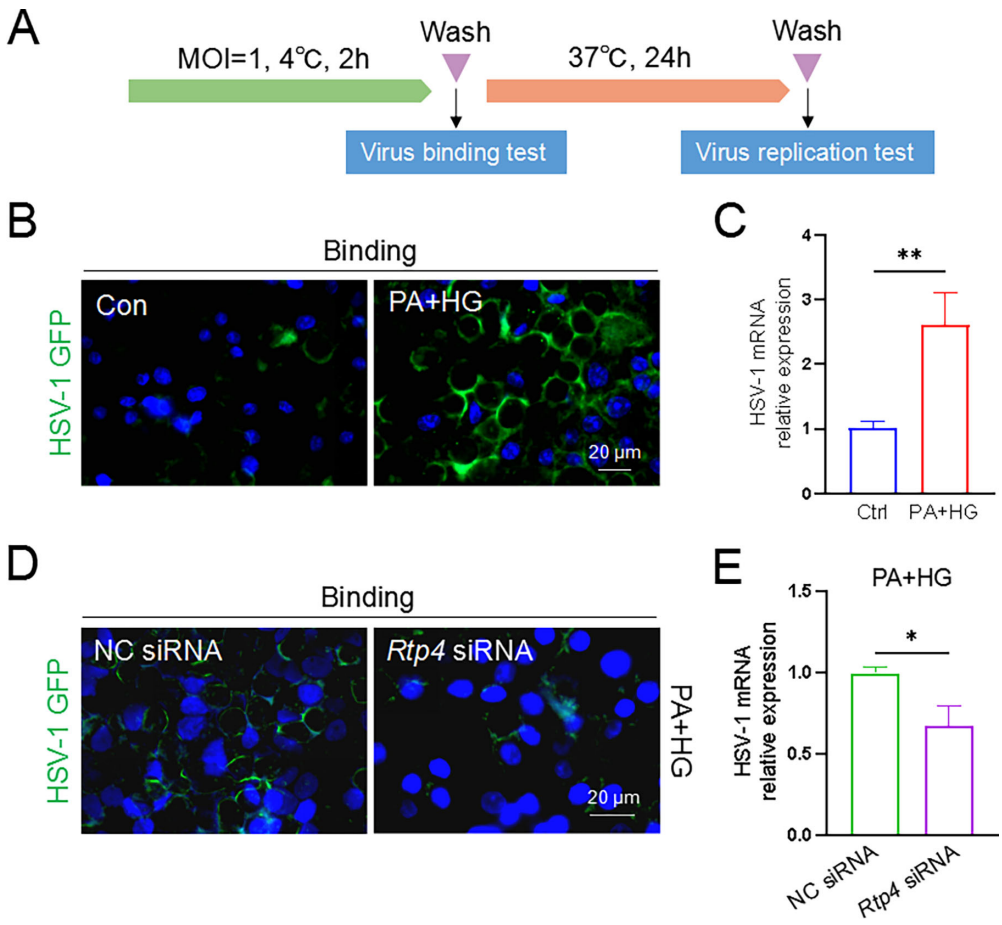

Figure 6. RTP4 participated in HSV-1 binding on HCEC cells. (**A**) A schematic of HSV-1 binding and replication assays in HCECs. The GFP-expressing H129-G4 HSV-1 strain of virus was applied. (**B**) In HCECs, viral binding was enhanced in the T2D group compared with the control group. HCECs were infected with the HSV-1 GFP virus (MOI = 1) and then stored at 4°C for 2 hours, washed, and fixed, and fluorescent signals of HSV-1 on the cell membrane were observed. (**C**) Incubation with 37°C for 24 hours following virus binding, quantitative PCR analysis of HSV-1 replication was assessed between control and T2D groups. (**D**) In the T2D cell model, *Rtp4* knockdown reduced the viral binding. (**E**) HSV-1 replication was evaluated between the NC siRNA-treated and the *Rtp4* siRNA-treated T2D groups. Incubation conditions are the same as in Figure 6C. NC, negative control. *Blue* for DAPI. $^{*}P < 0.05$, $^{**}P < 0.01$.

T2D mice and db/db mice, and this upregulation was also confirmed in the corneal epithelium of patients with T2D. HFD/STZ-induced T2D mice exhibited enhanced HSV-1 infection, accompanied by increased corneal opacity and upregulated HSV-1 virus transcripts. Furthermore, the HG/PA-induced T2D cell model revealed that increased RTP4 exacerbated HSV-1 infection by promoting HSV-1 binding to corneal epithelial cells. Conversely, *Rtp4* knockdown inhibited HSV-1 binding and consequently reduced infection. In T2D mice, *Rtp4* knockdown ameliorated the severity of infectious lesions, indicating enhanced corneal resistance to HSV-1. These results suggested that RTP4 may augment the susceptibility of T2D individuals to HSV-1, thereby offering a potential intervention target for the acute phase of infection in T2D.

T2D is widely recognized as a chronic inflammatory disease.[29] The corneas of patients with T2D exhibit sensory neurodegeneration, delayed repair, and immune dysregulation, rendering them vulnerable to infection.[30] However, the mechanism underlying patients' with T2D susceptibility to infection remains elusive. RNA-seq analysis of corneal epithelium revealed activation of innate immunity and an enhanced viral response in db/db mice. Innate immunity, serving as the first barrier against pathogen invasion, relies on the antiviral effect mediated by interferon-stimulated genes (ISGs) activated by interferons (IFNs).[31] Transcriptome analysis unveiled significant upregulation of ISGs, including *Rtp4*, *Isg15*, *Ifit1*, *Ifit3*, *Oas2*, and *Oas3*, in the corneal epithelium of db/db mice. This finding aligned with our observations in HFD/STZ-induced T2D mice, implying an enhanced antiviral capability. However, compared to control mice, T2D mice exhibited higher RTP4 expression levels, more severe corneal phenotypes, and increased viral replication following HSV-1 infection, suggesting a positive correlation between RTP4 expression and HSV-1 replication. Both in vivo and in vitro experiments further demonstrated that disruption of Rtp4 attenuated HSV-1 infection and replication. Corneas from *Rtp4*-deficient T2D mice displayed enhanced antiviral protection, indicating that RTP4 aggravates corneal HSV-1 infection. This finding is consistent with its role in suppressing experimental cerebral malaria in the mouse brain.[10] Despite numerous studies attributing an antiviral role to RTP4 against pathogens, such as SARS-CoV-2, Zika virus, and hepatitis C virus,[9,11,12] T2D may create an immune microenvironment conducive to HSV-1 infection, potentially exacerbated by RTP4.

Investigative Ophthalmology & Visual Science

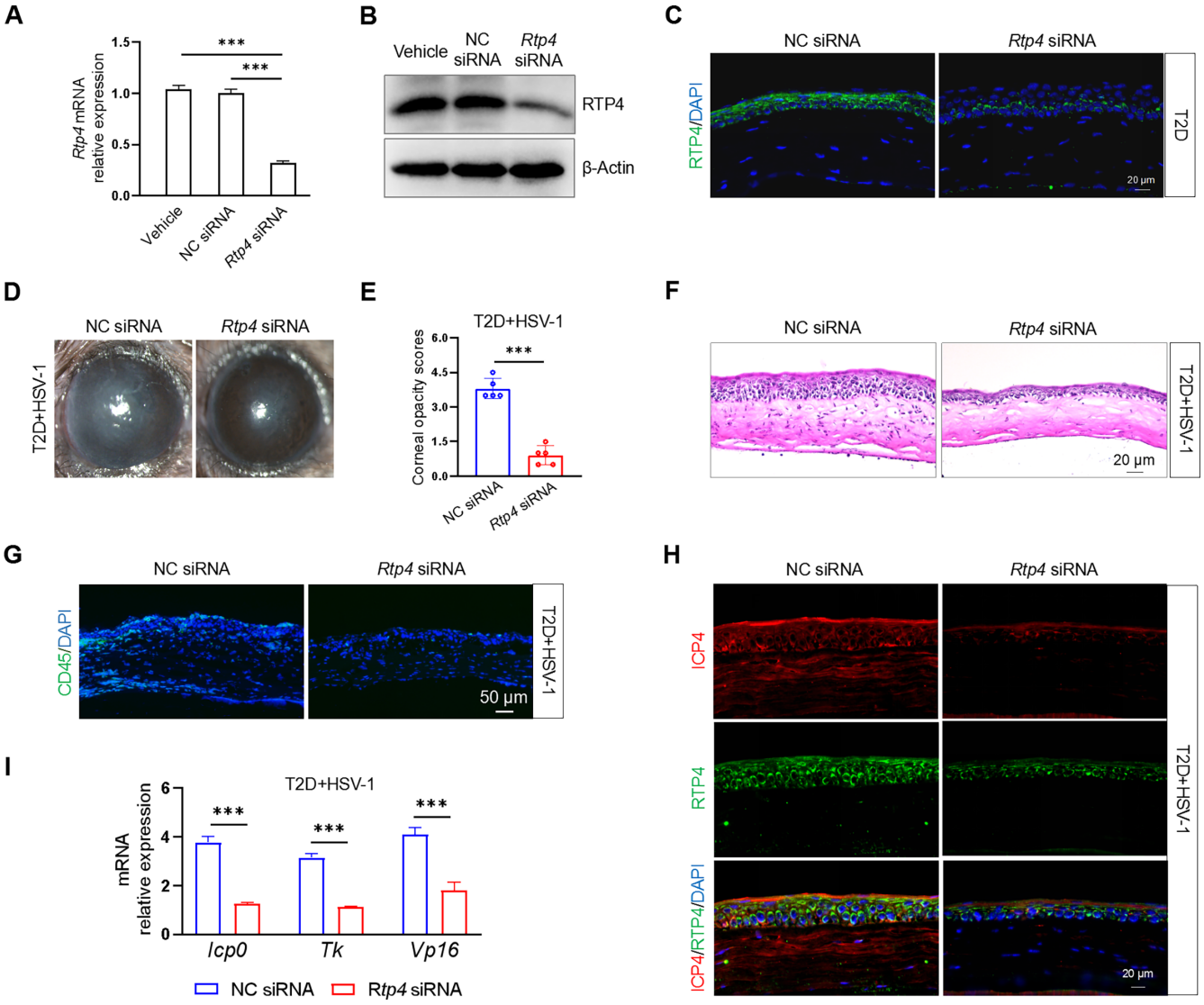

Figure 7. Therapeutic effect of *Rtp4* knockdown on corneal HSV-1 infection in T2D mice. Knockdown of mouse *Rtp4* by subconjunctival injection of siRNA was detected by quantitative PCR (**A**), Western blot (**B**), and immunofluorescence staining (**C**) in the cornea of T2D mice. (**D**) *Rtp4* knockdown ameliorated the corneal phenotype in T2D mice at 5 Dpi. (**E**) *Rtp4* knockdown decreased the corneal opacity scores in T2D mice at 5 Dpi. (**F**) H&E staining of corneal sections. (**G**) *Rtp4* knockdown reduced the infiltration of immune cells (CD45+). (**H**) Staining for ICP4 and RTP4 of corneal sections. (**I**) Quantitative PCR analysis of HSV-1 viral genes were assessed in T2D mice at 5 Dpi. The *m-Rpl5* served as an internal control. NC, negative control. ***$P < 0.001$.

We found that RTP4 was localized in the cytoplasm of corneal epithelial cells and was not detected in the cell membrane, which is consistent with previous reports of murine and human RTP4 localization in endoplasmic reticulum and Golgi apparatus.[32] Our data showed that RTP4 mediated the binding of HSV-1 to corneal epithelial cells, influencing viral entry. However, the mechanism by which RTP4 promotes HSV-1 binding to host cells is unclear. Given that HSV-1 binding to host cells requires specific cellular receptor proteins, such as TNFRSF14 and NECTIN1 as gD receptors, and MYH9, MAG, and PILRA as gB receptors,[33,34] we hypothesize that RTP4 may behave as a chaperone protein, facilitating the proper folding of these receptors and promoting their transport to the cell membrane. This process could enhance their cell surface expression and increase the binding of HSV-1 to corneal epithelial cells.

In addition to its role in viral replication, RTP4 has been linked to immune cell regulation in various cancers. In colorectal cancer, RTP4 is associated with resistance to immune checkpoint blockade, and silencing its expression can inhibit T lymphocyte recruitment.[35] In cutaneous melanoma, RTP4 has been identified as a novel prognostic hub gene that promotes neutrophil infiltration.[36] In mouse breast cancer, RTP4 mediates tumor cell sensitivity to antigen-dependent T-cell killing.[37] After HSV-1 infection, immunofluorescence staining for RTP4 and CD45 revealed that RTP4 was detected in a small number of immune cells (Supplementary Fig. S3, indicated by yellow arrowheads), suggesting that immune cells may be involved in mouse corneal HSV-1 infection. However, RTP4 was predominantly localized to corneal epithelial cells (see Supplementary Fig. S3), indicating that our results mainly reflect the role of corneal epithelial cells. The impact of RTP4 on corneal

Investigative Ophthalmology & Visual Science

immune cells and the significance of its expression in these cells warrant further investigation.

Diabetic individuals are prone to more severe and widespread infections.[38–40] However, whether they are more susceptible to HSV-1 is controversial. Previous studies have reported diabetes as a risk factor for herpetic keratitis, with a higher incidence rate in patients with T2D compared to non-diabetic individuals.[41,42] Additionally, the concentration of HSV-1 IgG in the serum of patients with diabetes was higher than that in non-diabetic individuals.[5] However, a study from Wills Eye Hospital found that T2D does not worsen HSK.[43] A recent retrospective study identified older age and diabetes as risk factors for poor outcomes in HSK, leading to visually significant corneal scarring.[6] Our results demonstrated that T2D exacerbated HSK lesions, characterized by higher corneal opacity scores, increased corneal edema, and greater HSV-1 virus transcripts, confirming the aggravating effect of T2D on acute HSV-1 infection.

Taken together, our findings indicated that RTP4 was upregulated in the corneal epithelium of T2D mice and exacerbated the infection phenotype by facilitating HSV-1 binding. Conversely, *Rtp4* knockdown effectively mitigated the degree of HSK lesions in T2D mice. This suggests that RTP4 may emerge as a potential intervention target for acute HSV-1 infection in T2D.

Acknowledgments

The authors thanks Jumin Zhou for providing the HSV-1 Mckrae strain, and Lihong Li and Erlin Wang for providing technical guidance on virus replication and titer determination.

Supported by the National Natural Science Foundation of China (82000851), the Natural Science Foundation of Shandong Province (ZR2020QH144, ZR2020QH236, and ZR2022MH026), the Taishan Scholar Program (tstp20221163), and the Qingdao Shinan District Science and Technology Plan Project (2022-2-018-YY).

Disclosure: **Y. Dai**, None; **S. Mao**, None; **X. Zang**, None; **H. Ge**, None; **J. Feng**, None; **Y. Wang**, None; **X. Qi**, None; **L. Yang**, None; **Q. Zhou**, None; **X. Wang**, None

References

1. Lobo AM, Agelidis AM, Shukla D. Pathogenesis of herpes simplex keratitis: the host cell response and ocular surface sequelae to infection and inflammation. *Ocul Surf*. 2019;17(1):40–49.
2. Paludan SR, Bowie AG, Horan KA, Fitzgerald KA. Recognition of herpesviruses by the innate immune system. *Nat Rev Immunol*. 2011;11(2):143–154.
3. Azher T, Yin XT, Tajfirouz D, Huang A, Stuart P. Herpes simplex keratitis: challenges in diagnosis and clinical management. *Clin Ophthalmol*. 2017;11:185–191.
4. Rowe AM, St. Leger AJ, Jeon S, Dhaliwal DK, Knickelbein JE, Hendricks RL. Herpes keratitis. *Prog Retin Eye Res*. 2013;32:88–101.
5. Sun Y, Pei W, Wu Y, Yang Y. An association of herpes simplex virus type 1 infection with type 2 diabetes. *Diabetes Care*. 2005;28(2):435–436.
6. Rosenberg CR, Abazari A, Chou TY, Weissbart SB. Comparison of comorbid associations and ocular complications in herpes simplex and zoster keratitis. *Ocul Immunol Inflamm*. 2022;30(1):57–61.
7. Safir M, Mimouni M. Atopic disease as a risk factor for recurrent herpetic keratitis. *Microorganisms*. 2024;12(1):220.
8. Behrens M, Bartelt J, Reichling C, Winnig M, Kuhn C, Meyerhof W. Members of RTP and REEP gene families influence functional bitter taste receptor expression. *J Biol Chem*. 2006;281(29):20650–20659.
9. Boys IN, Xu E, Mar KB, et al. RTP4 is a potent IFN-inducible anti-flavivirus effector engaged in a host-virus arms race in bats and other mammals. *Cell Host Microbe*. 2020;28(5):712–723.e9.
10. He X, Ashbrook AW, Du Y, et al. RTP4 inhibits IFN-I response and enhances experimental cerebral malaria and neuropathology. *Proc Natl Acad Sci USA*. 2020;117(32):19465–19474.
11. Kaur R, Tada T, Landau NR. Restriction of SARS-CoV-2 replication by receptor transporter protein 4 (RTP4). *Mbio*. 2023;14(4):e0109023.
12. Nielsen JR, Lazear HM. Antiviral effector RTP4 bats against flaviviruses. *Immunity*. 2020;53(6):1133–1135.
13. Nath S, Ghosh SK, Choudhury Y. A murine model of type 2 diabetes mellitus developed using a combination of high fat diet and multiple low doses of streptozotocin treatment mimics the metabolic characteristics of type 2 diabetes mellitus in humans. *J Pharmacol Toxicol Methods*. 2017;84:20–30.
14. Furman BL. Streptozotocin-induced diabetic models in mice and rats. *Curr Protoc Pharmacol*. 2015;70:5.47.1–5.47.20.
15. Cheng Y, Yu X, Zhang J, et al. Pancreatic kallikrein protects against diabetic retinopathy in KK Cg-Ay/J and high-fat diet/streptozotocin-induced mouse models of type 2 diabetes. *Diabetologia*. 2019;62(6):1074–1086.
16. Skovsø S. Modeling type 2 diabetes in rats using high fat diet and streptozotocin. *J Diabetes Investig*. 2014;5(4):349–358.
17. Coleman DL. Obese and diabetes: two mutant genes causing diabetes-obesity syndromes in mice. *Diabetologia*. 1978;14(3):141–148.
18. Suriano F, Vieira-Silva S, Falony G, et al. Novel insights into the genetically obese (ob/ob) and diabetic (db/db) mice: two sides of the same coin. *Microbiome*. 2021;9(1):147.
19. Feng J, Yang L, Ran L, et al. Loss of TRPM8 exacerbate herpes simplex keratitis infection in mice by promoting the infiltration of CD11b+ Ly6G+ cells and increasing the viral load in the cornea. *Invest Ophthalmol Vis Sci*. 2023;64(15):24.
20. Tian X, Wang T, Zhang S, et al. PEDF reduces the severity of herpetic simplex keratitis in mice. *Invest Ophthalmol Vis Sci*. 2018;59(7):2923–2931.
21. Montgomery ML, Callegan MC, Fuller KK, Carr DJJ. Ocular glands become infected secondarily to infectious keratitis and play a role in corneal resistance to infection. *J Virol*. 2019;93(16):e00314–e00319.
22. Bu J, Yu J, Wu Y, et al. Hyperlipidemia affects tight junctions and pump function in the corneal endothelium. *Am J Pathol*. 2020;190(3):563–576.
23. Song Y, Zhang H, Zhu Y, et al. Lysozyme protects against severe acute respiratory syndrome coronavirus 2 infection and inflammation in human corneal epithelial cells. *Invest Ophthalmol Vis Sci*. 2022;63(6):16.
24. He DX, Tam SC. Trichosanthin affects HSV-1 replication in Hep-2 cells. *Biochem Biophys Res Commun*. 2010;402(4):670–675.
25. He D, Mao A, Li Y, et al. TRPC1 participates in the HSV-1 infection process by facilitating viral entry. *Sci Adv*. 2020;6(12):eaaz3367.
26. Zhao L, Chen R, Qu J, et al. Establishment of mouse model of neurotrophic keratopathy through TRPV1 neuronal ablation. *Exp Eye Res*. 2024;240:109814.

27. Wang X, Qu M, Li J, Danielson P, Yang L, Zhou Q. Induction of fibroblast senescence during mouse corneal wound healing. *Invest Ophthalmol Vis Sci*. 2019;60(10):3669–3679.
28. Wang X, Sun J, Wang Z, Li C, Mao B. EphA7 is required for otic epithelial homeostasis by modulating Claudin6 in Xenopus. *Biochem Biophys Res Commun*. 2020;526(2):375–380.
29. Nikolajczyk BS, Jagannathan-Bogdan M, Shin H, Gyurko R. State of the union between metabolism and the immune system in type 2 diabetes. *Genes Immun*. 2011;12(4):239–250.
30. Yu FSX, Lee PSY, Yang L, et al. The impact of sensory neuropathy and inflammation on epithelial wound healing in diabetic corneas. *Prog Retin Eye Res*. 2022;89:101039.
31. Iwasaki A, Pillai PS. Innate immunity to influenza virus infection. *Nat Rev Immunol*. 2014;14(5):315–328.
32. Fujita W, Yokote M, Gomes I, Gupta A, Ueda H, Devi LA. Regulation of an opioid receptor chaperone protein, RTP4, by morphine. *Mol Pharmacol*. 2019;95(1):11–19.
33. Spear P.G. Entry of alphaherpesviruses into cells. *Semin Virol*. 1993;4(3):167–180.
34. Lathe R, Haas JG. Distribution of cellular HSV-1 receptor expression in human brain. *J Neurovirol*. 2017;23(3):376–384.
35. Yamamoto Y, Shimada S, Akiyama Y, et al. RTP4 silencing provokes tumor-intrinsic resistance to immune checkpoint blockade in colorectal cancer. *J Gastroenterol*. 2023;58(6):540–553.
36. Li Y, Qi J, Yang J. RTP4 is a novel prognosis-related hub gene in cutaneous melanoma. *Hereditas*. 2021;158(1):22.
37. Wroblewska A, Dhainaut M, Ben-Zvi B, et al. Protein barcodes enable high-dimensional single-cell CRISPR screens. *Cell*. 2018;175(4):1141–1155.e16.
38. Guembel HO, Ohrloff C. Opportunistic infections of the eye in immunocompromised patients. *Ophthalmologica*. 1997;211(Suppl 1):53–61.
39. Lauri C, Leone A, Cavallini M, Signore A, Giurato L, Uccioli L. Diabetic foot infections: the diagnostic challenges. *J Clin Med*. 2020;9(6):1779.
40. Mansoor H, Tan HC, Lin MTY, Mehta JS, Liu YC. Diabetic corneal neuropathy. *J Clin Med*. 2020;9(12):3956.
41. Wang B, Yang S, Zhai HL, et al. A comparative study of risk factors for corneal infection in diabetic and non-diabetic patients. *Int J Ophthalmol*. 2018;11(1):43–47.
42. Kaiserman I, Kaiserman N, Nakar S, Vinker S. Herpetic eye disease in diabetic patients. *Ophthalmology*. 2005;112(12):2184–2188.
43. Kosker M, Hammersmith KM, Nagra PK, Nassef AH, Rapuano CJ. The association between diabetes and herpes simplex eye disease. *Ocul Immunol Inflamm*. 2018;26(1):125–129.

Investigative Ophthalmology & Visual Science